Developmental Biology **209,** 143–158 (1999)



# Rib Truncations and Fusions in the Sp$^{2H}$ Mouse Reveal a Role for Pax3 in Specification of the Ventro-lateral and Posterior Parts of the Somite

**Deborah J. Henderson, Simon J. Conway,[1] and Andrew J. Copp[2]**

*Neural Development Unit, Institute of Child Health, University College London, 30 Guilford Street, London WC1N 1EH, United Kingdom*

**The *splotch (Pax3)* mouse mutant serves as a model for developmental defects of several types, including defective migration of dermomyotomal cells to form the limb musculature. Here, we describe abnormalities of the ribs, neural arches, and acromion in *Sp$^{2H}$* homozygous embryos, indicating a widespread dependence of lateral somite development on *Pax3* function. Moreover, the intercostal and body wall muscles, derivatives of the ventrolateral myotome, are also abnormal in *Sp$^{2H}$* homozygotes. *Pax3* is expressed in the dermomyotome, but not in either the sclerotome or the myotome, raising the possibility that *Pax3*-dependent inductive influences from the dermomyotome are necessary for early specification of lateral sclerotome and myotome. Support for this idea comes from analysis of gene expression markers of lateral sclerotome (*tenascin-C* and *scleraxis*) and myotome (*myogenin, MyoD,* and *Myf5*). All exhibit ventrally truncated domains of expression in *Sp$^{2H}$* homozygotes, potentially accounting for the rib and intercostal muscle truncations. In contrast, the medial sclerotomal marker *Pax1* is expressed normally in mutant embryos, arguing that *Pax3* is not required for development of the medial sclerotome. Most of the somitic markers show ectopic expression in anteroposterior and mediolateral dimensions, suggesting a loss of definition of somite boundaries in *splotch* and explaining the rib and muscle fusions. An exception is *Myf5,* which is not ectopically expressed in *Sp$^{2H}$* homozygotes, consistent with the previous suggestion that *Pax3* and *Myf5* function in different pathways of skeletal myogenesis. PDGF$\alpha$ and its receptor are candidates for mediating signalling between myotome and sclerotome. We find that both genes are misexpressed in *Sp$^{2H}$* embryos, suggesting that PDGF$\alpha$/PDGFR$\alpha$ may function downstream of *Pax3,* accounting for the close similarities between the *splotch* and *Patch* mutant phenotypes. Our findings point to additional regulatory functions for the Pax3 transcription factor, apart from those already demonstrated for development of the neural tube, neural crest, and dermomyotome.** 

## INTRODUCTION

The paraxial mesoderm of the vertebrate embryo contains the progenitor cells of the skeletal muscles of the trunk and limbs, the dermis, and the cartilage of the developing vertebrae and ribs (reviewed by Christ and Ordahl, 1995; Christ *et al.*, 1998). At approximately E9.0 in the developing mouse embryo, the paraxial mesoderm starts to become subdivided to form the segmentally arranged, epithelial somites. Each somite differentiates by the breakdown of its ventromedial wall to form the sclerotome, whereas its dorsolateral wall remains epithelial, comprising the dermomyotome. A mesenchymal population of cells located within the cavity of the epithelial somite, the somitocoel, contributes to the lateral sclerotome as development proceeds (Huang *et al.*, 1994).

The dermomyotome subsequently undergoes an epitheliomesenchymal transformation, with cells delaminating from both dorsal and ventral margins to form the myotome. Cells delaminating from the dorsomedial lip of the dermomyotome migrate beneath its medial surface and give rise to the epaxial (deep back) muscles, whereas cells located at the ventrolateral lip of the dermomyotome form the hypaxial (limb and body wall) musculature. The vertebral bodies arise from the medial part of the sclerotome. Less well understood is the origin of the ribs and neural arches, although these structures are generally thought to arise from the lateral sclerotome. Recent analysis using the quail–chick marking system has suggested that the lateral dermomyotome may give rise to the distal part of the ribs and the intercostal muscles

[1] Current address: Institute of Molecular Medicine & Genetics, Developmental Biology Program, Room CA 4008, Medical College of Georgia, Augusta, GA 30912-2640.

[2] To whom correspondence should be addressed. Fax: 44-171 831 4366. E-mail: a.copp@ich.ucl.ac.uk.

0012-1606/99 $30.00

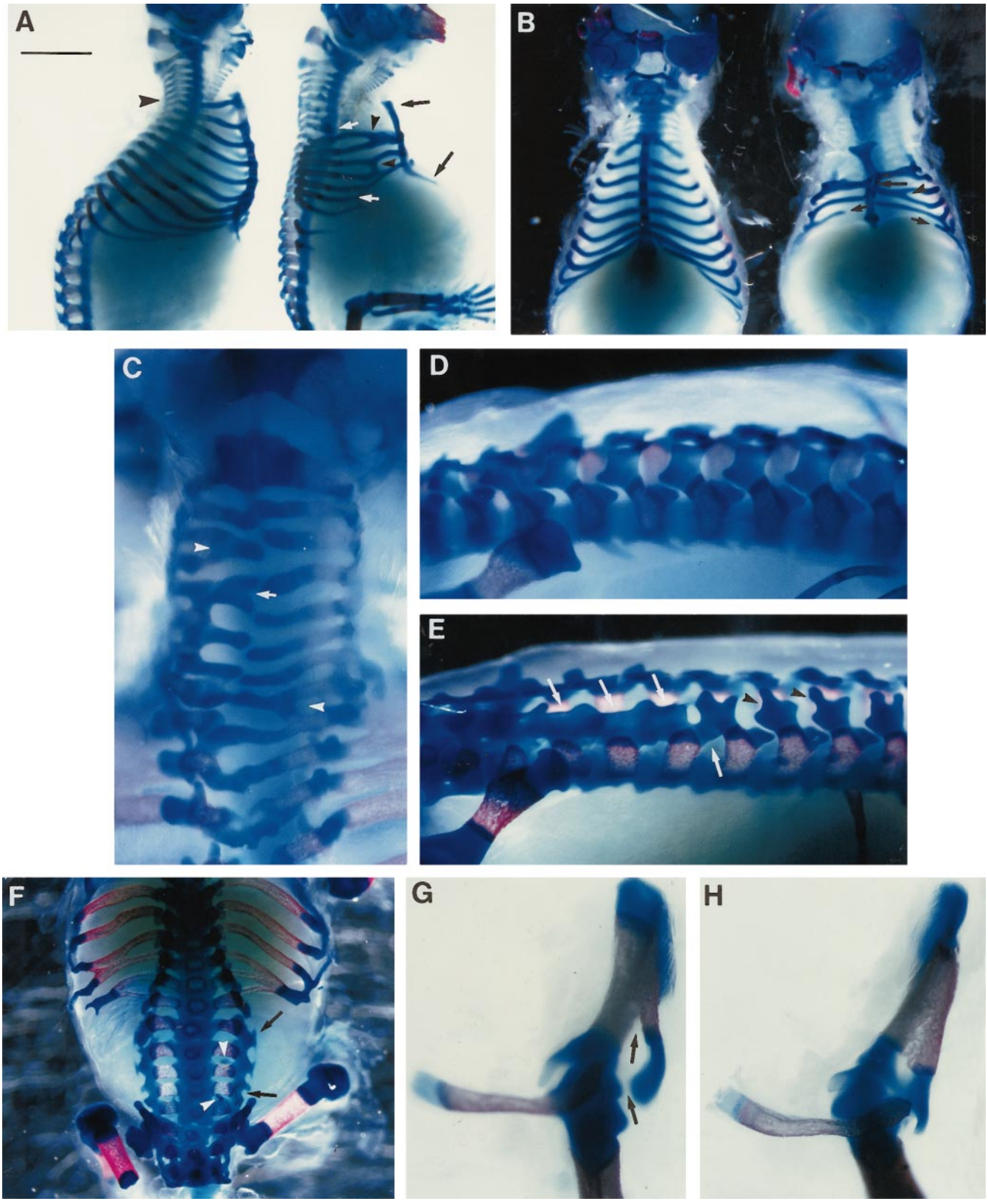


**FIG. 1.** Skeletal defects in E18.5 $Sp^{2H}/Sp^{2H}$ foetuses. Bright-field (A, G, H) and dark-field (B–F) micrographs of Alcian blue- and alizarin S-stained preparations. (A) Lateral views of wild type (left; $n = 12$) and $Sp^{2H}$ homozygous (right; $n = 12$) foetuses showing rib truncations

(Kato and Aoyama, 1998). In contrast, a previous study using the quail–chick system found that somitocoel cells contribute to the ribs (Huang *et al.,* 1994). It seems possible, from these studies, that a proportion of the lateral sclerotome is derived from somitocoel cells that themselves originate in the lateral portion of the somitic wall (i.e., the future dermomyotome).

Recent work in the mouse has revealed a number of genes, including platelet-derived growth factor receptor $\alpha$ (*PDGFR*$\alpha$), *paraxis, Myf-5,* and *Pax1,* that play vital roles in development of the paraxial mesoderm. Mutations in these genes result in abnormalities in one or other of the paraxial mesodermal lineages (Braun *et al.,* 1992; Timmons *et al.,* 1994; Burgess *et al.,* 1996; Soriano, 1997). Another key gene in somite development is *Pax3,* which is disrupted in the *splotch* allelic group of mouse mutants (Epstein *et al.,* 1991; Goulding *et al.,* 1994). *Pax3* is a member of the Pax family of homeobox-containing transcription factors and exhibits developmentally regulated expression in the central nervous system, paraxial mesoderm, and early migrating neural crest (Goulding *et al.,* 1991b; Conway *et al.,* 1997b). This pattern of gene expression mirrors the range of developmental defects seen in *splotch* mutant mice which include (1) neural tube closure defects, specifically exencephaly and spina bifida; (2) absence of limb musculature, resulting from faulty migration of muscle precursor cells from the dermomyotome; and (3) neural crest-related defects, including reduced or absent dorsal root ganglia, decreased numbers of Schwann cells, pigmentation abnormalities, and failure of cardiac outflow tract septation (Franz, 1992a; Chalepakis *et al.,* 1993a; Conway *et al.,* 1997a). The failure of dermomyotomal muscle progenitors to migrate into the limb bud in the *splotch* mouse has been the subject of detailed studies which indicate a key role for *Pax3* in the regulation of skeletal muscle formation (Bober *et al.,* 1994; Goulding *et al.,* 1994; Maroto *et al.,* 1997; Tajbakhsh *et al.,* 1997).

In the present paper, we describe abnormalities of the ribs, neural arches, and acromion of the scapula in *splotch* ($Sp^{2H}$) homozygotes. We also find abnormalities of the intercostal and ventral body wall muscles in $Sp^{2H}/Sp^{2H}$ embryos. These skeletal and muscle defects can be traced back to abnormalities of somite development, first seen at E10.5–11.5, when the somite is becoming compartmentalised. The expression of genes specific for the dermomyotome, myotome, and lateral sclerotome are truncated dorsoventrally in $Sp^{2H}$ homozygotes, even though *Pax3* is not expressed in either the myotome or the sclerotome. Moreover, the expression domains of several genes are fused anterior–posteriorly in the myotome and lateral sclerotome, suggesting incorrect specification of these somite compartments in $Sp^{2H}$ mutants. Our findings point to a hitherto unknown function for *Pax3* in developmental regulation within the ventrolateral part of the somite.

## MATERIALS AND METHODS

### *Mouse Strains and Embryos*

$Sp^{2H}$ is a radiation-induced allele at the *splotch* locus that arose on the C3H/101 background (Beechey and Searle, 1986). A heterozygote $Sp^{2H}/+$ female, obtained from the MRC Radiobiology Unit (Harwell, UK), was mated with a CBA/Ca male and the offspring were mated *inter se* to found a randomly bred colony. $Sp^{2H}$ heterozygotes, identified by the presence of a white belly spot, were mated together to provide litters containing $Sp^{2H}/Sp^{2H}$ homozygotes. Midday on the day of finding a copulation plug was designated embryonic day 0.5 (E0.5). Pregnant females were killed by cervical dislocation and the embryos/foetuses were placed in Dulbecco's modified Eagle's medium (Gibco, UK) containing 10% foetal calf serum. The yolk sac and amnion were opened and the umbilical cord was cut. The yolk sac was processed for PCR genotyping using *Pax3* primers as described previously (Epstein *et al.,* 1991b).

### *Whole-Mount Skeletal Staining*

Foetuses at E18.5 were dissected free from the amnion and placed at −20°C for 15 min. The skin was then carefully removed under a dissecting microscope to allow penetration of the fixative and stains. Foetuses were fixed for 3–4 days in 20%

(white arrows) and fusions (small arrowheads) in the mutant embryo. $Sp^{2H}$ homozygotes lack the normal curvature of the cervical spine seen in wild-type littermates (large arrowhead). The sternum is truncated inferiorly and appears "free" superiorly (black arrows), owing to the incomplete nature of the most rostral ribs. (B) Ventral views of wild-type (left) and $Sp^{2H}$ homozygous (right) foetuses, showing the asymmetrical truncations (small arrows) and fusions (arrowhead) of the ribs in the mutant foetus. The sternum is bifurcated (large arrow) and the ribs are fused to the sternum at only two or three points on each side in the $Sp^{2H}$ homozygote. (C) Neural arch fusions as seen in dorsal view of the cervical region of a $Sp^{2H}/Sp^{2H}$ foetus. Rostral is to the top. The neural arches are asymmetrically bifurcated (arrow) and fused rostrocaudally (arrowheads). (D and E) Lumbar region of the vertebral column in wild-type (D) and $Sp^{2H}/Sp^{2H}$ (E) foetuses. Rostral is to the right. The mutant foetus, which did not have a spina bifida, shows extensive rostrocaudal fusions of the neural arches (arrows). The neural arches adjacent to the region of fusion are misshapen (arrowheads). (F) Anteroposterior fusions of the neural arches, spanning up to six vertebrae, in the lumbar region of a $Sp^{2H}/Sp^{2H}$ foetus (arrows). This foetus had a large spina bifida, and the neural arches are widely displaced from the midline. Ectopic cartilage is present in the region of the fused neural arches (arrowheads). (G and H) Scapulas from wild-type (G) and $Sp^{2H}/Sp^{2H}$ (H) foetuses. The distal end of the acromion is clearly distinct from the scapula in the wild-type foetus (arrows in G), whereas it is fused with the blade of the scapula in the mutant foetus (H). Scale bar represents A and B, 3 mm; C, 0.7 mm; D, E, G, and H, 0.9 mm; F, 1.5 mm.

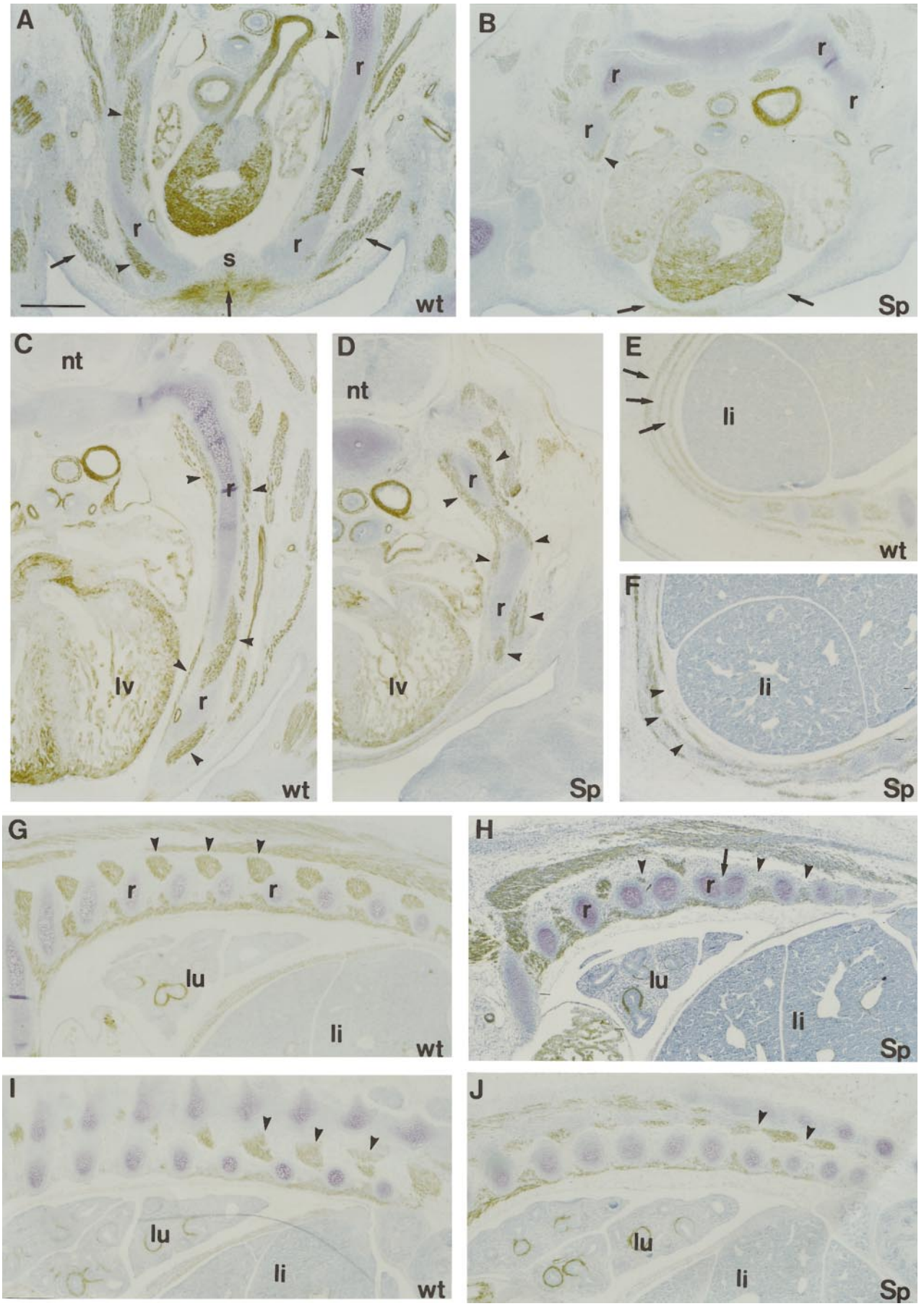
A
r
r
s
r
wt
B
r
r
r
r
Sp
C
nt
r
lv
r
wt
D
nt
r
r
lv
Sp
E
li
wt
F
li
Sp
G
r
r
lu
li
wt
H
r
r
lu
li
Sp
I
lu
li
wt
J
lu
li
Sp

glacial acetic acid/95% ethanol containing 0.3 mg/ml Alcian blue 8GX, followed by dehydration in 100% ethanol for 2 days, with several changes. They were then slowly rehydrated to water. The bone was stained with 0.2 mg/ml alizarin red S in 0.5% KOH for up to 1 h. The tissues were cleared in 20% glycerol in 1% KOH with frequent changes of solution, until the nonskeletal tissues became transparent, and then transferred through a series of 25, 50, and 75% glycerol in 1% KOH. The embryos were stored in 100% glycerol at 4°C and photographed using a Zeiss SV11 stereomicroscope.

## *Immunocytochemistry for Skeletal Muscle*

Foetuses were collected at E13.5–E14.5, fixed in 4% paraformaldehyde (PFA), and processed for embedding in paraffin wax. Transverse and longitudinal sections were cut at 8-$\mu$m thickness. The sections were dewaxed in Histoclear (National Diagnostics) and rehydrated through an alcohol series to deionized water. The sections were treated with 3% $H_2O_2$ for 5 min to block endogenous peroxidase, washed in Tris-buffered saline (TBS) for 5 min, and overlaid with 10% foetal calf serum (FCS) in TBS for 15 min to block nonspecific epitopes. Monoclonal antibody to $\alpha$-smooth muscle actin (Sigma) was applied overnight at 4°C, at a dilution of 1/400 (in 2% FCS in TBS). Next morning, the sections were washed three times in TBS, and a biotinylated rabbit anti-mouse secondary antibody (1/400 dilution in 2% FCS in TBS) (Dako) was applied for 1 h at room temperature. The sections were washed three times in TBS, then avidin–biotin complex linked to horseradish peroxidase (Dako) was applied for 30 min at room temperature. Following washing in TBS, the presence of peroxidase was revealed by staining using the substrate diaminobenzidine hydrochloride. Negative controls, using 2% mouse serum substituted for the primary antibody, yielded no staining in all cases. Sections were counterstained with toluidine blue, dehydrated, and mounted in DPX before photography using an Axiophot (Zeiss) photomicroscope.

## *Generation of cDNA Clones by RT-PCR*

Total RNA was isolated from E10.5 CBA/Ca embryos using TRIzol (Gibco BRL). One microgram of RNA was used in the reverse transcriptase reaction according to the methodology of Kawasaki (1990) using random hexanucleotides (Gibco BRL). Primers were designed to the published sequences of *tenascin-C* (base pairs 16–40 and 423–447; GenBank), *paraxis* (base pairs 490–510 and 911–931; Burgess *et al.*, 1995) and *scleraxis* (base pairs 615–635 and 1039–1059; Cserjesi *et al.*, 1995). Thirty cycles of amplification were carried out and fragments of the expected size were synthesised, ligated into the pGEM-T vector (Promega), and sequenced to confirm their identity. Other cDNA probes were *Pax3* (from Peter Gruss, Gottingen), *Pax1* (from Kenji Imai, Munich), *myogenin*, *Myf-5* and *MyoD* (from Simon Hughes, London), and platelet-derived growth factor $\alpha$ (*PDGF*$\alpha$) and *PDGFR*$\alpha$ (from Mark Mercola, Boston).

## *Whole-Mount in Situ Hybridisation*

The methodology of Wilkinson (1992) was followed. Briefly, embryos were fixed in 4% PFA and dehydrated through a methanol series before being stored in 100% methanol prior to processing. The embryos were rehydrated, treated with proteinase K, refixed, and hybridised at 70°C overnight with digoxygenin-labelled riboprobes. The following morning the embryos were washed at high stringency at 70°C and then incubated with anti-digoxygenin antibody for 1–3 days at 4°C (Boehringer Mannheim). Sites of hybridisation were revealed by incubation in the presence of 0.34 mg/ml nitroblue tetrazolium chloride and 0.18 mg/ml 5-bromo-4-chloro-3-indolylphosphate (Gibco BRL). The reaction was stopped and the embryos were stored for several days at 4°C to allow background to fade, before being photographed with a Zeiss SV11 stereomicroscope and processed for sectioning. In all cases sense controls were carried out with no evidence of nonspecific hybridisation.

For Vibratome sectioning, the embryos were placed in a mixture of 0.45% gelatine, 27% albumen, 18% glucose in PBS which was solidified by the addition of 1/10 volume of 30% glutaraldehyde. Embryos were sectioned at 50 $\mu$m using a Vibratome Series 1000 and sections were stored under coverslips in PBT:glycerol (1:1) at 4°C until photography using an Axiophot (Zeiss) photomicroscope. Comparison between different markers was performed on transverse sections at a level just caudal to the forelimb bud, unless otherwise stated.

**FIG. 2.** Immunohistochemistry for $\alpha$ smooth muscle actin (brown staining) in sections through E13.5 wild-type (A, C, E, G, I; $n = 5$) and $Sp^{2H}/Sp^{2H}$ (B, D, F, H, J; $n = 5$) foetuses, photographed using bright-field optics. Sections counterstained with toluidine blue. (A and B) Transverse sections through the upper thoracic region of wild-type (A) and $Sp^{2H}/Sp^{2H}$ (B) foetuses. The ribs (r) extend ventrally to join the sternum (s) in the wild-type foetus. Intercostal muscles are visible internal and external to the ribs (arrowheads) and ventral body wall muscles are located external to the intercostal muscles (arrows). The $Sp^{2H}/Sp^{2H}$ foetus (B) shows severe ventral truncation of the ribs and with almost no evidence of intercostal muscle development (arrowhead). Ventral body wall muscles are also drastically reduced (arrows). (C and D) Transverse sections through wild-type (C) and $Sp^{2H}/Sp^{2H}$ (D) foetuses at the lower thoracic level. The ribs extend almost to the ventral midline of the wild-type foetus, with intercostal muscles on internal and external surfaces of the ribs (arrowheads). At this axial level, the ribs extend a similar distance ventrally in $Sp^{2H}/Sp^{2H}$ foetuses (D), although they are misshapen. Intercostal muscles are evident flanking the ribs (arrowheads). (E and F) Transverse sections showing the abdominal wall muscles surrounding the liver (li) in wild-type (E) and $Sp^{2H}/Sp^{2H}$ (F) foetuses. Three complete layers of muscle can be seen in both wild-type (arrows in E) and mutant foetuses, but the layers are interrupted in the mutant foetus (arrowheads in F). (G–J) Longitudinal sections through the thoracic region of wild-type (G and I) and $Sp^{2H}/Sp^{2H}$ (H and J) foetuses. Rostral is to the left. The ribs and intercostal muscles (arrowheads) are arranged in a regular, alternating, segmental manner in wild-type foetuses, whereas mutant foetuses have an irregular arrangement in which neighbouring ribs are sometimes fused (arrow in H) and the intercostal muscles may be reduced in size or missing (arrowheads in H) or fused to each other (arrowheads in J). Other abbreviations: lu, lung; lv, left ventricle of heart; nt, neural tube. Scale bar represents 360 $\mu$m.

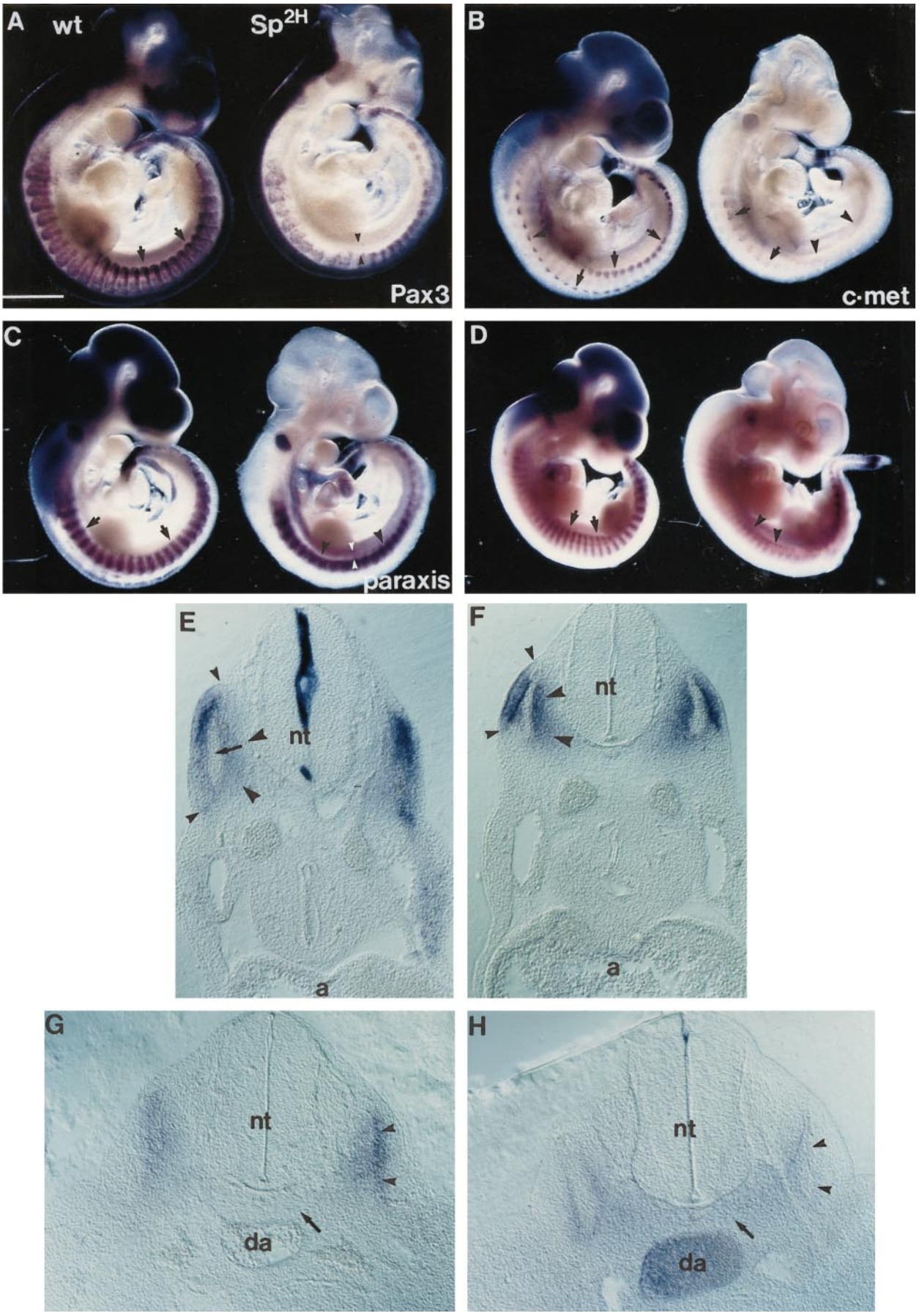
A
wt
Sp2H
Pax3
B
c-met
C
paraxis
D
E
nt
a
F
nt
a
G
nt
da
H
nt
da

## RESULTS

### *Skeletal Defects in the $Sp^{2H}$ Mutant*

Although 50% of $Sp^{2H}$ homozygotes die of heart failure around E14.5, the remaining heterozygotes survive to birth (Conway *et al.*, 1997a). We collected surviving $Sp^{2H}$ homozygotes at E18.5 and used Alcian blue and alizarin red S, which stain cartilage and bone, respectively, to examine their skeletal structure.

$Sp^{2H}/Sp^{2H}$ foetuses lack the normal concave curvature of the cervical spine which can be seen in wild-type littermates (Fig. 1A). The most dramatic skeletal defects, however, affect the ribs, manifesting as fusions and bifurcations, often involving multiple ribs (Figs. 1A and 1B). These defects appear to be fully penetrant among homozygous mutant foetuses that survive to E18.5. The fusions and bifurcations are found both proximally and distally and are asymmetrical, occurring with equal frequency on both sides of the sternum. Partial truncations also affect the distal part of the ribs with the proximal part remaining in all cases (Fig. 1A). The extent of these truncations is difficult to assess, however, because of the fusions which make individual ribs difficult to follow. These is no evidence for reduced numbers of ribs in $Sp^{2H}$ homozygotes. In contrast, supernumerary ribs, arising from the sixth and seventh cervical vertebrae, have been seen in several $Sp^{2H}/Sp^{2H}$ foetuses. Frequently, the four or five most anterior ribs fused as a block to the more caudal ribs, leaving the anterior part of the sternum "free" (Fig. 1A). As the sternum is also shortened caudally (Fig. 1A), this results in an abnormal number of floating ribs. In some $Sp^{2H}/Sp^{2H}$ foetuses the sternal bands remain unfused, giving the sternum a bifurcated appearance (Fig. 1B).

Abnormalities in the neural arches are also seen in 100% of $Sp^{2H}/Sp^{2H}$ foetuses that survive to E18.5. In the cervical region, the neural arches are misshapen and may be fused rostrocaudally, often in an asymmetrical pattern (Fig. 1C). In the lumbar region more extensive fusions are evident, spanning several vertebral bodies (Figs. 1E–1F). These fusions are found irrespective of whether the foetus manifests a spina bifida, suggesting they do not result from failure of neural tube closure. Ectopic cartilage is frequently found in the region of the lumbar neural arch fusions (Fig. 1F), although the vertebral bodies are apparently normal.

The acromion, the bone that extends from the spine of the scapula, is completely fused to the scapula in all mutant embryos (Figs. 1G and 1H). The remainder of the skeleton in $Sp^{2H}/Sp^{2H}$ foetuses appears normal, with two exceptions. First, much of the cranial skeleton is missing from foetuses with exencephaly, as the failure of cranial neural tube closure prevents normal skeletal development in the region of the defect. Second, although the limb bones are of normal size and shape, bowing of the long bones is not apparent (data not shown). This may be a consequence of the lack of limb musculature rather than a primary defect in limb bone formation since there is no known defect in osteogenesis per se in *splotch* mutants. Thus, a number of specific defects are present in the skeleton of $Sp^{2H}/Sp^{2H}$ foetuses, all of which affect tissues of somitic origin.

### *The Musculature of the Trunk Is Abnormal in the $Sp^{2H}$ Mutant*

In view of the severe patterning defects observed in the ribs and neural arches of the $Sp^{2H}$ mutant embryos, we next examined the trunk musculature of $Sp^{2H}/Sp^{2H}$ embryos at

**FIG. 3.** Whole-mount *in situ* hybridisation using digoxygenin-labelled probes for the dermomyotomal markers *Pax3* (A), *c-met* (B), and *paraxis* (C–H). (A–D) Intact wild-type (left) and $Sp^{2H}/Sp^{2H}$ (right) embryos at E10.5–11.5; (E–H) Vibratome sections of the whole-mount *paraxis* preparations. Nonspecific trapping of probe can be seen in the brain ventricles of wild-type embryos (A–D) and in the lumen of the neural tube in E. (A) *Pax3* transcripts are detected in the somites and neural tube of both wild-type ($n = 10$) and $Sp^{2H}/Sp^{2H}$ ($n = 10$) embryos at E10.5. In wild-type embryos, *Pax3* is expressed most intensely in the ventral/posterior domain of the somites (arrows), whereas this domain of expression is truncated ventrally in $Sp^{2H}/Sp^{2H}$ embryos (between the small arrowheads). (B) E10.5 wild-type ($n = 6$) and $Sp^{2H}/Sp^{2H}$ ($n = 6$) embryos showing *c-met* expression. The most dorsal and ventral parts of the dermomyotome express *c-met* in wild-type (arrows), whereas expression is absent from the ventral part of the dermomyotome along the entire body axis in $Sp^{2H}/Sp^{2H}$ embryos (arrowheads). Expression is retained in the dorsal part of the somite at rostral levels of the body axis in mutant embryos (arrows). (C) *Paraxis* expression in E10.5 wild type ($n = 6$) and $Sp^{2H}/Sp^{2H}$ ($n = 6$) embryos. Transcripts are detectable in a segmental pattern in the somites of wild-type embryos (arrows), whereas expression in $Sp^{2H}/Sp^{2H}$ embryos is truncated ventrally (between the small white arrowheads) and fused anterior–posteriorly (arrowhead). (D) *Paraxis* expression at E11.5 in wild-type ($n = 6$) and $Sp^{2H}/Sp^{2H}$ ($n = 6$) embryos. Discrete bands of expression extend dorsoventrally in wild-type embryos (arrows), whereas these expression domains are truncated in $Sp^{2H}/Sp^{2H}$ embryos (arrowheads). (E) E10.5 wild-type embryo, sectioned at the level of the heart, showing *paraxis* expression in the dermomyotome (between the small arrowheads) and, at lower intensity, in the sclerotome (large arrowheads). The myotome does not express *paraxis* (arrow). (F) E10.5 $Sp^{2H}/Sp^{2H}$ embryo sectioned at a level equivalent to that of (E). The dermomyotomal domain of *paraxis* expression (between small arrowheads) is truncated dorsoventrally, whereas the mutant sclerotome (large arrowheads) expresses *paraxis* more intensely than in the wild type. (G and H) *paraxis* expression in E11.5 wild-type (G) and $Sp^{2H}/Sp^{2H}$ (H) embryos, sectioned at the level of the forelimb bud. Expression in wild-type embryos is maintained in the dermomyotome (arrowheads), but is down-regulated in the medial sclerotome at this stage (arrow). In contrast, *paraxis* expression is not present in the dermomyotome of the mutant embryo (arrowheads), whereas it is expressed ectopically in the sclerotome (arrow). Abbreviations: a, atrium of heart; da, dorsal aorta; nt, neural tube. Scale bar represents A, 1.1 mm; B and C, 1.5 mm; D, 2.2 mm; E–H, 175 $\mu$m.

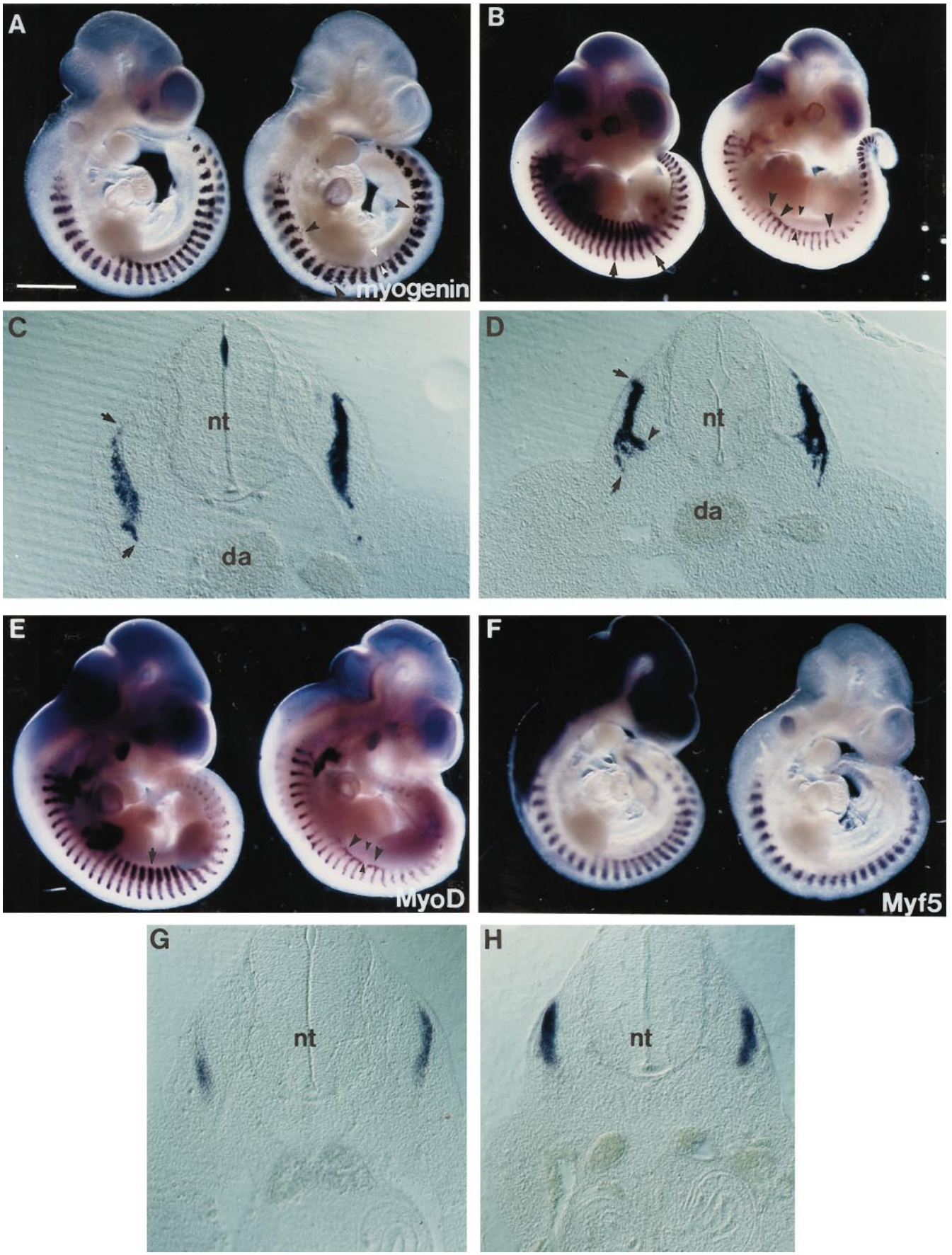
A
myogenin
B
C
nt
da
D
nt
da
E
MyoD
F
Myf5
G
nt
H
nt

E13.5–14.5, concentrating particularly on the intercostal and ventral body wall muscles.

Immunocytochemistry for $\alpha$ smooth muscle actin in transverse and longitudinal sections of E13.5 $Sp^{2H}/Sp^{2H}$ and wild-type littermates revealed a range of defects in the trunk musculature of mutant embryos. The intercostal muscles are reduced or missing at various levels of the body axis in mutant embryos (Figs. 2A–2D, 2G, and 2H). Interestingly, the degree of rib truncation correlates with the development of the intercostal muscles within a single embryo. In cases in which individual ribs are truncated or their trajectory is diverted, there is little evidence of intercostal muscle development (Fig. 2B). Conversely, where individual ribs are present, intercostal muscles are also found, flanking the ribs (Fig. 2D). This suggests an interrelationship between rib and intercostal muscle development. Longitudinal sections reveal anterior–posterior fusions of intercostal muscles in mutant embryos, which are never seen in wild-type littermates (Figs. 2I and 2J).

The abdominal wall muscles are also abnormal in mutant embryos. Although three layers of abdominal wall muscle can be seen in both $Sp^{2H}/Sp^{2H}$ and wild-type embryos, the layers are discontinuous in the mutants and do not follow the smooth lines seen in wild-type (Figs. 2E and 2F). Sections through the limb confirm the lack of limb musculature (data not shown).

### *Truncation of the Somite as Shown by Markers of the Dermomyotome, Myotome, and Sclerotome*

Gene expression markers for the dermomyotome, myotome, and sclerotome were examined in $Sp^{2H}$ homozygotes and wild-type littermates at E10.5–11.5 in order to trace the developmental origins of the defects in somite derivatives. Examination of the dermomyotomal markers *Pax3* (Fig. 3A) and *c-met* (Fig. 3B) confirmed previous findings that the dermomyotome is ventrally truncated in the $Sp^{2H}$ mutant at E10.5 (Daston *et al.*, 1996). In contrast, we observed little dorsal truncation of the Pax3 expression domain in mutant embryos. To extend this analysis, we examined the expression of *paraxis*, a basic helix-loop-helix transcription factor that is expressed in the dermomyotome and, to a lesser extent, in the sclerotome (Burgess *et al.*, 1995). Analysis of embryos at E10.5–11.5, by whole-mount *in situ* hybridisation, showed dorsoventral truncation of the expression domain in $Sp^{2H}/Sp^{2H}$ embryos (Figs. 3C and 3D). Sectioning these embryos confirmed ventral truncation of the dermomyotome at all levels of the body axis in the $Sp^{2H}/Sp^{2H}$ embryos compared with wild-type littermates (Figs. 3E and 3F and data not shown).

Next we examined the expression of the myotomal markers *myogenin*, *Myf5*, and *MyoD* in $Sp^{2H}$ litters by whole-mount *in situ* hybridisation at E10.5–11.5. The expression domains of *myogenin* (Figs. 4A–4D), *MyoD* (Fig. 4E), and *Myf5* (Figs. 4F–4H) are all truncated dorsoventrally in $Sp^{2H}$ homozygotes compared with wild-type littermates.

Expression of *tenascin-C* and *scleraxis* mRNA marks the lateral domain of the sclerotome (Cserjesi *et al.*, 1995). At E10.5, both markers are expressed at very low levels with no identifiable differences between wild-type and mutant embryos (data not shown). At E11.5, abnormalities of expression can be seen in $Sp^{2H}$ homozygotes, with ventral truncation of the expression domains of both genes in the flank of the $Sp^{2H}$ homozygotes (Figs. 5A and 5B). Vibratome sectioning of wild-type embryos confirms that *tenascin-C* (Fig. 5C) and *scleraxis* (data not shown) are both expressed in the lateral sclerotome, in a pattern distinct from that of *Pax1*, which marks the medial sclerotome around the notochord (Fig. 5G). The *tenascin-C* expression domain is truncated dorsally and ventrally in $Sp^{2H}$ homozygotes, with maintenance of intense expression in medially located cells (Fig. 5D). At E12.5, the expression of *tenascin-C* marks the rib primordia (Fig. 5E). The expression domain does not extend as far ventrally in the $Sp^{2H}$ homozygotes. Thus, the expression of gene markers reveals truncation of the lateral sclerotome compartment in *splotch* mutants. In contrast, there are no apparent differences between wild-type and

**FIG. 4.** Whole-mount *in situ* hybridisation using digoxygenin-labelled probes for the myotomal markers *myogenin* (A–D), *MyoD* (E), and *Myf5* (F, G, and H). (A, B, E, and F) Intact wild-type (left) and $Sp^{2H}/Sp^{2H}$ (right) embryos at E10.5–11.5; (C, D, G, and H) Vibratome sections of the whole-mount preparations. (A) *myogenin* is expressed in the somites of wild-type ($n = 6$) and $Sp^{2H}/Sp^{2H}$ ($n = 6$) embryos at E10.5 of gestation. The expression domain is truncated ventrally (between small white arrowheads) in mutants compared with wild-type littermates. Moreover, positive cells are present outside of the normal expression domain (black arrowheads), making the somites appear ragged. (B) At E11.5, the expression domain of *myogenin* has extended ventrally into the flank of wild-type ($n = 6$) embryos (arrows), whereas the expression domain remains truncated ventrally in mutant littermates ($n = 6$; between small arrowheads). Expression domains between individual somites are often fused ventrally in $Sp^{2H}/Sp^{2H}$ embryos (large arrowheads). (C and D) Sections of E10.5 wild-type (C) and $Sp^{2H}/Sp^{2H}$ (D) embryos at the level of the forelimb confirm the presence of *myogenin* transcripts in the myotome of wild-type embryos (arrows), whereas, in mutant embryos, the expression domain is truncated ventrally (arrows), and there are ectopic myogenin-expressing cells in the sclerotome (arrowhead). (E) By E11.5, the expression domain of *MyoD* has extended ventrally into the flank of wild-type embryos ($n = 6$; arrow), whereas the expression domain is truncated ventrally in $Sp^{2H}/Sp^{2H}$ littermates ($n = 6$; between small arrowheads), with ventral fusions between individual somites (large arrowheads). (F) *Myf5* is expressed in the somites of wild-type ($n = 6$) and $Sp^{2H}/Sp^{2H}$ ($n = 6$) embryos at E10.5. The expression domain is truncated ventrally in mutant embryos. (G and H) Vibratome sectioning reveals *Myf5* expression in the E10.5 wild-type myotome, whereas the *Myf5* expression domain is truncated ventrally in $Sp^{2H}/Sp^{2H}$ embryos (H). There is no evidence of ectopic *Myf5*-expressing cells in the mutant sclerotome in either whole mounts (F) or sections (G and H). Abbreviations: da, dorsal aorta; nt, neural tube. Scale bar represents A and F, 1.1 mm; B, 2.2 mm; C, D, G, and H, 175 $\mu$m; E, 1.5 mm.

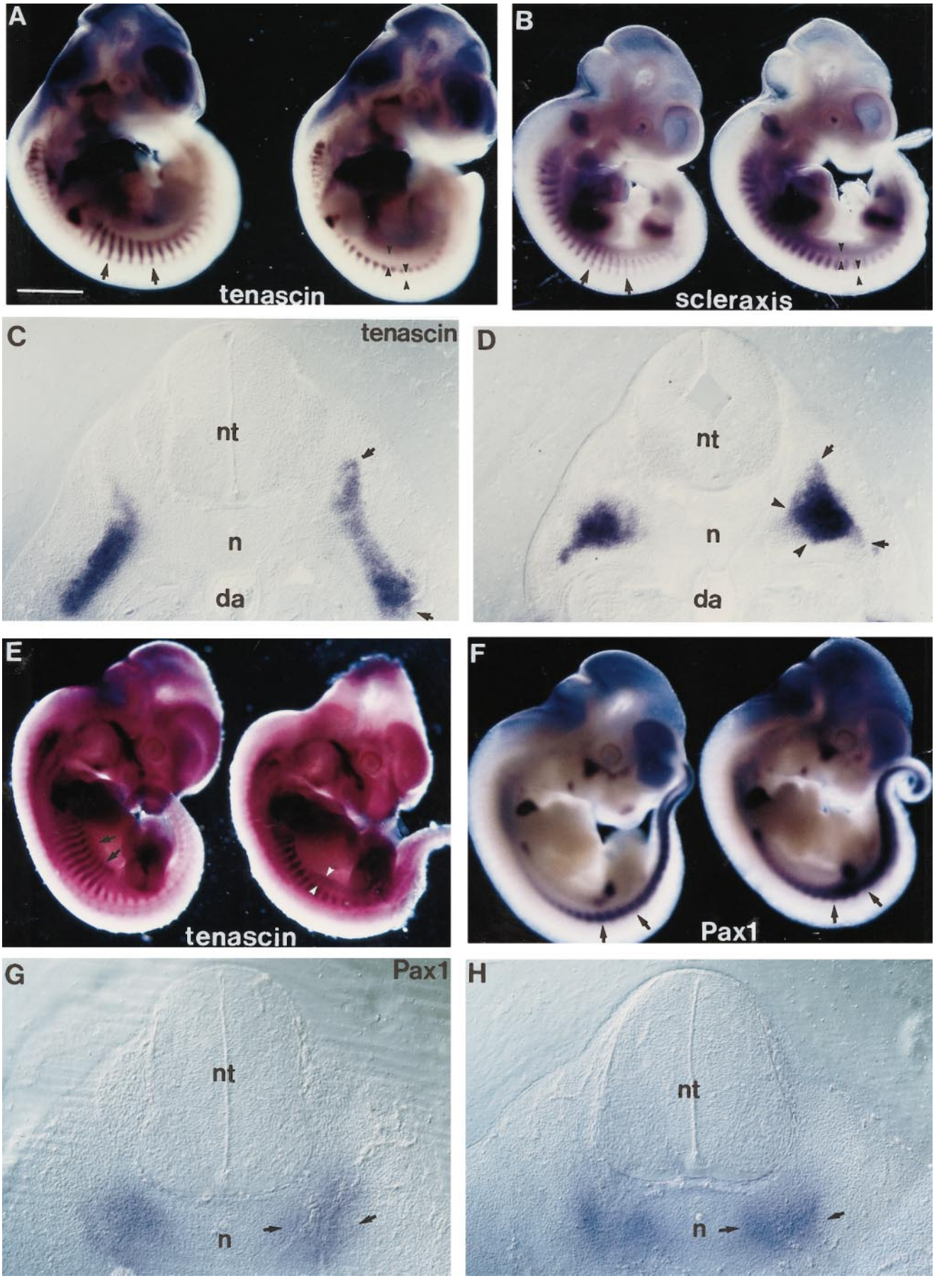
A
tenascin
B
scleraxis
C
tenascin
nt
n
da
D
nt
n
da
E
tenascin
F
Pax1
G
Pax1
nt
n
H
nt
n

mutant embryos in the expression of the medial sclerotome marker *Pax1* (Figs. 5F–5H).

### *Ectopic Expression of Somite Markers in $Sp^{2H}$ Homozygotes*

In addition to ventral truncation of the three somite compartments, whole-mount *in situ* hybridisation reveals further abnormalities in the patterning of somitic gene expression in $Sp^{2H}$ homozygotes at E10.5–11.5. Whereas *Pax3* and *c-met* are confined to their normal expression domains (Figs. 3A and 3B), *paraxis* is expressed ectopically in $Sp^{2H}/Sp^{2H}$ embryos at both E10.5 and E11.5. This produces an almost continuous band of *paraxis* expression along the flank of mutant embryos at E10.5, in contrast to the discrete segmental pattern of expression seen in control embryos (Fig. 3C). Transverse sections of E10.5 embryos reveal that *paraxis* is expressed at higher levels in the sclerotome of mutant than in that of wild-type embryos (Figs. 3E and 3F). By E11.5, the divergence of the *paraxis* expression pattern between mutant and wild-type is even more apparent (Fig. 3D): *paraxis* is still expressed in the dermomyotome of wild-type embryos (Fig. 3G), whereas expression in the dermomyotome of mutant embryos is markedly less intense. In contrast, *paraxis* continues to be expressed in the sclerotome of $Sp^{2H}$ homozygotes, although it is now absent from this site in wild-type embryos (Figs. 3G and 3H). In summary, $Sp^{2H}$ mutants show expression of *paraxis* in the wrong somite domain and with abnormal rostrocaudal organisation.

Analysis of the myotomal markers *myogenin* and *MyoD* also reveals ectopic expression of these markers outside their normal somitic domains in mutant embryos. At E10.5, *myogenin* is expressed outside the discrete somitic blocks seen in wild-type embryos, giving the mutant somites a ragged appearance (Fig. 4A). Transverse Vibratome sections of these embryos reveal ectopic expression of *myogenin* in the sclerotomal compartment of the $Sp^{2H}$ homozygotes, but not in wild-type controls (Figs. 4C and 4D), suggesting that the myotome is disorganised in both rostrocaudal and mediolateral dimensions. By E11.5, the expression domains of both *myogenin* (Fig. 4B) and *MyoD* (Fig. 4E) in adjacent somites are fused ventrally in a rostrocaudal direction. In contrast, examination of *Myf5* expression at E10.5–11.5 (Figs. 4F–4H and data not shown) shows that, despite the ventral truncation of the expression domain, there is no ectopic expression outside of the myotome, although the expression domain does appear to be slightly expanded mediolaterally.

Lateral sclerotomal markers are also expressed outside their normal domains in $Sp^{2H}$ homozygotes. Examination of sectioned E11.5 embryos shows mediolateral expansion of the *tenascin-C* expression domain (Figs. 5C and 5D). These data suggest that the boundaries of the different somite compartments are poorly defined in $Sp^{2H}$ homozygotes and that cells are able to migrate outside of their normal somite compartments as a consequence of this defect.

### *PDGFα and its receptor are abnormally expressed in the somites of $Sp^{2H}$ homozygotes*

The severe patterning defects in the derivatives of the lateral sclerotome, and the gene expression abnormalities in markers of the dermomyotome, myotome, and sclerotome, suggest a defect of signalling between the different somite compartments in $Sp^{2H}$ mutants. A number of growth factors, including PDGF$\alpha$ and members of the transforming growth factor $\beta$ (TGF$\beta$) and fibroblast growth factor (FGF) families, have been implicated in the regulation of lateral sclerotome development. Moreover, the close similarity between defects in $Sp^{2H}$ and PDGFR$\alpha$ mutant embryos (Soriano, 1997) suggests that there could be abnormalities in the PDGF$\alpha$ ligand–receptor interaction in the $Sp^{2H}$ mutant.

We examined expression of *PDGFα*; and its receptor by whole-mount *in situ* hybridisation at E10.5 and E11.5. The somites of $Sp^{2H}$ homozygotes exhibit truncated expression of *PDGFα* compared with wild-type littermates (Figs. 6A and 6B). Additionally, there is anterior–posterior fusion of expression domains ventrally at E11.5 (Fig. 6B). Thus, *PDGFα*-expressing cells are not restricted by the normal somite boundaries in $Sp^{2H}$ embryos. Vibratome sections

**FIG. 5.** Whole-mount *in situ* hybridisation using digoxygenin-labelled probes for the sclerotomal markers *tenascin-C* (A, C, D, and E), *scleraxis* (B), and *Pax1* (F–H). (A, B, E, and F) Intact wild-type (left) and $Sp^{2H}/Sp^{2H}$ (right) embryos at E11.5–12.5; (C, D, G, and H) Vibratome sections of the whole-mount preparations. (A) *tenascin-C* is expressed segmentally in the flank of wild-type ($n = 10$) embryos at E11.5 (arrows). This expression domain is truncated both dorsally and ventrally in $Sp^{2H}/Sp^{2H}$ embryos ($n = 10$; between small arrowheads). (B) *scleraxis* is also segmentally expressed in wild-type ($n = 4$) at E11.5 (arrows), with dorsal and ventral truncation of the expression domain in mutant embryos ($n = 4$; between small arrowheads). (C and D) *tenascin-C* whole-mount preparations at E11.5 sectioned through the thoracic region, just caudal to the forelimb. Wild-type embryos (C) show expression in the lateral sclerotome (between arrows), whereas this domain of expression is truncated ventrally (between arrows), but expanded mediolaterally (arrowheads), in $Sp^{2H}/Sp^{2H}$ embryos (D). (E) By E12.5, the *tenascin-C* expression domain has extended dorsoventrally in wild-type embryos ($n = 3$) and now prefigures the development of the ribs (arrows). $Sp^{2H}/Sp^{2H}$ embryos ($n = 3$) show ventral truncation of this expression domain (between small white arrowheads). (F) *Pax1* is expressed along the flank of both wild-type ($n = 6$) and $Sp^{2H}/Sp^{2H}$ embryos ($n = 6$) at E11.5 (arrows). (G and H) Sections of the E11.5 whole-mount embryos show that *Pax1* is expressed in the medial sclerotome (arrows), surrounding the notochord, in a distribution that does not overlap with *tenascin-C* and that does not differ between wild-type (G) and $Sp^{2H}/Sp^{2H}$ (H) embryos. Abbreviations: n, notochord; nt, neural tube; da, dorsal aorta. Scale bar represents A and F, 1.5 mm; B, 1.1 mm; C, D, G, and H, 175 $\mu$m; E, 1.8 mm.

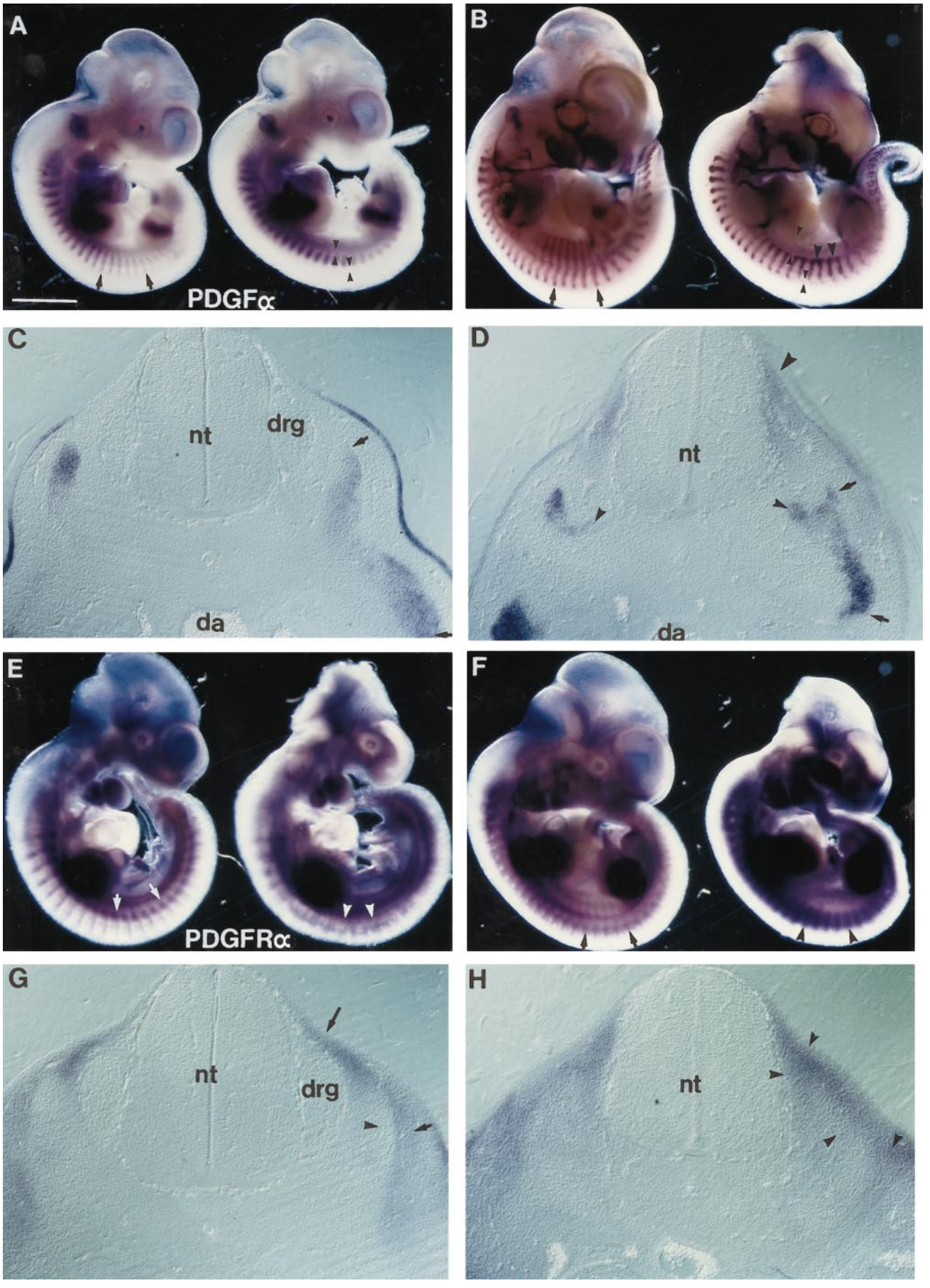
A
PDGFα
B
C
nt
drg
da
D
nt
da
E
PDGFRα
F
G
nt
drg
H
nt

(Figs. 6C and 6D) show that the myotomal expression of *PDGFα* is truncated dorsally and ventrally and that positively stained cells are present ectopically in the sclerotome. Ectopic *PDGFα* expression is also found in $Sp^{2H}$ homozygotes in the mesoderm adjacent to the dorsal part of the neural tube, a location from which it is absent in wild-type embryos (Figs. 6C and 6D). These findings confirm that *PDGFα* is expressed appropriately for a factor involved in signalling from the myotome to the sclerotome and show, moreover, that it is aberrantly expressed in $Sp^{2H}/Sp^{2H}$ embryos.

The receptor for PDGFα is normally expressed in the dermomyotome and sclerotome of the developing somite (Orr-Urtreger and Lonai, 1992). At E10.5, *PDGFRα* expression is much less discrete in $Sp^{2H}$ mutant embryos than in wild-type littermates (Fig. 6E), with transcripts detectable throughout the somite, rather than mainly in the posterior part of the somite, as in wild-type embryos (Fig. 6E). By E11.5, there appears to be higher levels of *PDGFRα* expression in the $Sp^{2H}$ mutant embryos, and again the expression is found throughout the somite, in contrast to the more restricted expression pattern in wild-type (Figs. 6F–6H). Thus, regional organisation of *PDGFRα* gene expression appears to be lost in $Sp^{2H}$ mutant embryos.

In conclusion, we find that anterior–posterior patterning in the ventrolateral part of the somite is severely disorganised in the $Sp^{2H}$ mutant. This is highlighted by the abnormal patterns of gene expression observed for markers of the various somite compartments in midgestation embryos. In contrast, specification of the medial sclerotome appears normal in mutant embryos. These disturbances of regional gene expression foreshadow later developmental defects in derivatives of the lateral part of the somite.

## DISCUSSION

In the present study we describe rib and neural arch abnormalities in the $Sp^{2H}$ mouse mutant, in addition to the neural tube, neural crest, and limb muscle defects that are already well recognised. These findings have recently been confirmed, in an independent study by Tremblay *et al.* (1998). *Pax3*, the gene mutated in $Sp^{2H}$, is initially expressed throughout the unsegmented paraxial mesoderm but, as the somite differentiates, it is down-regulated in the newly formed sclerotome and is not expressed in the myotome as it delaminates from the dermomyotome (Goulding *et al.*, 1994). We studied gene expression markers of the dermomyotome, myotome, and sclerotome in an effort to determine to what extent each somite compartment is disrupted by the absence of functional *Pax3*. We find a loss of spatial organisation in the somites of $Sp^{2H}$ homozygotes which may result in aberrant signalling between somite compartments and defective anterior–posterior patterning of skeletal and muscle elements.

### *Skeletal Derivatives of the Lateral Somite Are Abnormal in $Sp^{2H}$ Mutants*

We found that the ribs of $Sp^{2H}$ mutant embryos are severely abnormal, with multiple fusions and truncations and the presence of supernumerary cervical ribs. In addition, the neural arches are misshapen and fused in the cervical and lumbar regions and the acromion is fused to the scapula. All of these defects result from abnormalities in derivatives of the lateral somite and point to a specific disturbance in the patterning of this domain during $Sp^{2H}/Sp^{2H}$ development. Our study complements the recent work of Kato and Aoyama (1998), which suggests that the lateral dermomyotome may be the source of rib precursors.

Gene markers can be used to differentiate between cells of the medial and lateral sclerotome, as well as the dermomyotome. *Pax1* and *Pax9* mark the medial sclerotome, adjacent to the neural tube and surrounding the notochord (Deutsch *et al.*, 1988; Neubüser *et al.*, 1995), whereas *scleraxis* initially marks the lateral sclerotome, only later appearing in the medial sclerotome (Cserjesi *et al.*, 1995). *Tenascin-C* expression appears to be specific for the cells of

**FIG. 6.** Whole-mount *in situ* hybridisation using digoxygenin-labelled probes for *PDGFα* (A–D) and *PDGFRα* (E–H). (A, B, E, and F) Intact wild-type (left) and $Sp^{2H}/Sp^{2H}$ (right) embryos at E10.5–11.5; (C, D, G, and H) Vibratome sections of the whole-mount preparations. (A) *PDGFα* is expressed in a segmental pattern in the flank of wild-type ($n = 6$) embryos at E10.5 (arrows). This expression domain is truncated dorsally and ventrally in $Sp^{2H}/Sp^{2H}$ embryos ($n = 6$; between small arrowheads). (B) By E11.5, the *PDGFα* expression domain has extended ventrally in wild-type embryos ($n = 6$), whereas it is markedly truncated (between small arrowheads), with anterior–posterior fusions (large arrowheads) in $Sp^{2H}/Sp^{2H}$ littermates ($n = 6$). (C and D) Sections of whole-mount embryos at E11.5 show expression of *PDGFα* in the myotome (between arrows) of wild-type embryos (C), whereas the expression domain is truncated in the myotome (between arrows) of $Sp^{2H}/Sp^{2H}$ embryos (D), with ectopic expression in the sclerotome (small arrowheads) and in the dorsal mesoderm (large arrowhead). (E) *PDGFRα* is expressed in the posterior part of the somite of wild-type embryos at E10.5 ($n = 6$; arrows), whereas, in $Sp^{2H}/Sp^{2H}$ embryos ($n = 6$), *PDGFRα* is expressed ectopically throughout the somite (arrowheads). (F) At E11.5, *PDGFRα* continues to be expressed in the posterior part of each somite of wild-type embryos ($n = 6$; arrows), whereas $Sp^{2H}/Sp^{2H}$ embryos ($n = 6$) exhibit more intense expression that is distributed throughout the somite (arrowheads). (G and H) Sections of E11.5 wild-type embryos (G) reveal *PDGFRα* expression in the dermomyotome (small arrow) and in the dorsal mesoderm (large arrow). The myotome no longer expresses *PDGFRα* at this stage (arrowhead). In contrast, *PDGFRα* is expressed ectopically throughout the somites of $Sp^{2H}/Sp^{2H}$ embryos (H), with a generally higher intensity of transcripts (arrowheads). Abbreviations: da, dorsal aorta; drg, dorsal root ganglia; nt, neural tube. Scale bar represents A and E, 1.1 mm; B, 1.6 mm; C, D, G, and H, 175 $\mu$m; F, 1.5 mm.

the lateral sclerotome and by E12.5 can be seen marking the developing ribs. Analysis of $Sp^{2H}$ embryos reveals abnormalities in the expression of lateral sclerotomal markers, with medial markers apparently unaffected. Both *tenascin-C* and *scleraxis* show ventrally truncated expression domains compared with normal controls, whereas expression of *Pax1* does not differ between mutant and wild-type. This finding is consistent with previous suggestions that genes expressed in the medial and lateral part of the sclerotome, and the development of the structures that arise from these regions, are regulated independently. Genes expressed in the medial sclerotome, such as *Pax1*, are known to be under control of signals from the notochord, principally *sonic hedgehog* (Fan and Tessier-Lavigne, 1994). Much less is known about the signals that regulate the lateral part of the sclerotome (reviewed by Tajbakhsh and Spörle, 1998), although candidates include factors produced by the lateral plate mesoderm and surface ectoderm.

Our findings of defects in the ribs and neural arches in the $Sp^{2H}$ mutant can be interpreted in two ways. If these structures are derived from the lateral sclerotome, as has previously been thought (Huang *et al.*, 1994), then our data suggest that the dermomyotome, where *Pax3* is expressed, may be involved in regulating development of the lateral sclerotome. *Pax3* could regulate the expression of a signalling molecule that induces rib and neural arch development, either directly or through a second signal in the myotome. Alternatively, *Pax3* might be required to maintain development of the ventrolateral dermomyotome and, hence, permit signalling from dermomyotome/myotome to lateral sclerotome. If, however, the distal parts of the ribs are derived directly from ventrolateral dermomyotome, without involvement of lateral sclerotome (Kato and Aoyama, 1998), then the ventral truncation of the dermomyotome in the $Sp^{2H}/Sp^{2H}$ embryo can explain the rib truncations observed later in development. The absence of the ventrolateral dermomyotome in the $Sp^{2H}$ mutant embryos may result in a dearth of cells capable of forming distal rib structures, resulting in a truncated-rib phenotype. It is more difficult to explain the abnormalities of neural arches and acromion in $Sp^{2H}/Sp^{2H}$ embryos on the basis of a purely dermomyotomal defect. Kato and Aoyama (1998) did not report defects in these structures when the dermomyotome was extirpated, making it seem unlikely that these are also derivatives of the lateral dermomyotome. Additional extirpation and transplantation studies are needed to investigate this question further.

### *Origin of Defects of Intercostal and Body Wall Musculature in splotch*

It is well established that the limb muscles are missing from *splotch* mutants (Franz *et al.*, 1993; Bober *et al.*, 1994; Daston *et al.*, 1996). Tajbakhsh *et al.* (1997) extended this analysis of *splotch* musculature and demonstrated deficiencies in the muscles of the ventral body wall, diaphragm, and tongue (Ordahl and Le Douarin, 1992; Christ and Ordahl, 1995). We have shown that the intercostal muscles also show patterning abnormalities. Earlier in development, myotomal markers are ventrally truncated in the $Sp^{2H}$ mutant. In addition, cells expressing myotomal markers are found outside of their normal expression domain, in the sclerotome. *Pax3* may be specifically required for correct specification of the ventral myotome, or alternatively, the truncation of the myotome might result from the earlier loss of the ventral dermomyotome. Kato and Aoyama (1998) have suggested that the intercostal muscles are derived from the dermomyotome along with the distal rib precursors, raising the possibility that ventral truncation of the dermomyotome in the $Sp^{2H}$ mutant is directly responsible for the observed abnormalities in intercostal muscle development.

### *Myotome Formation Is Essential for Induction of Rib Precursors*

A number of mouse mutants, for example those lacking *Myf5* and *Pax1*, have rib truncations as a component of their phenotype. The *Myf5* null mouse has severe distal truncations such that all but the most proximal part of the rib is absent (Braun *et al.*, 1992). *Myf5* is expressed initially in the dorsal myotome, which is derived from the dorsomedial region of the dermomyotome. It then goes on to be expressed throughout the myotome (Smith *et al.*, 1994; Rudnicki and Jaenisch, 1995; Cossu *et al.*, 1996). Since *Myf5* is not expressed in the precursors of the distal rib, this demonstrates that myotome formation is essential for development of the ribs. This idea is supported by the finding that *myogenin*, expressed under the control of *Myf5* regulatory elements, can rescue rib development in *Myf5* null embryos (Wang *et al.*, 1996). Thus, it is the presence of the myotome, not the expression of *Myf5* per se, that is essential for rib formation.

These findings suggest that signalling between the myotome and the rib precursor cells may be essential for rib development, perhaps mediated by growth factors, including FGF-4, FGF-6, TGF$\beta$2, and PDGF$\alpha$ (Grass *et al.*, 1996; Soriano, 1997). Indeed *FGF-4* and *-6* mRNAs are absent from the myotome of mice lacking *Myf5* (Grass *et al.*, 1996). Although these factors can all induce cartilage formation *in vitro* (Tucker *et al.*, 1993; Grass *et al.*, 1996; Soriano, 1997) only the disruption of the PDGF$\alpha$ signalling pathway has been shown to result in rib truncations (Soriano, 1997). Significantly, embryos lacking PDGFR$\alpha$ have a skeletal phenotype very similar to that of $Sp^{2H}$ homozygotes, with multiple rib fusions and bifurcations that vary in extent and occurrence on either side of the sternum (Soriano, 1997). The PDGFR$\alpha$ null mice resemble *splotch* mutants in other ways, with extensive fusions of the neural arches, failure of fusion of the sternal bands, and poor development of the acromion, as well as neural tube and neural crest defects. In addition, the myotomes are fused ventrally, in an anterior–posterior direction (Soriano, 1997), as in $Sp^{2H}$ homozygotes.

*PDGFR$\alpha$* is expressed in the dermomyotome and the sclerotome, whereas the *PDGF$\alpha$* ligand is expressed in the myotome (Orr-Urtreger and Lonai, 1992), raising the possi-

bility that these molecules might be involved in signalling between the dermomyotome, the myotome, and the lateral sclerotome. We find that both *PDGFα* and its receptor are ectopically expressed in the somites of $Sp^{2H}$ homozygotes. In addition, unlike the other myotomal markers *myogenin, MyoD,* and *Myf5, PDGFα* is truncated both dorsally and ventrally in the $Sp^{2H}$ mutant somites, supporting the idea that its expression is required for induction of the lateral sclerotome markers *tenascin-C* and *scleraxis,* which also show dorsal and ventral truncations of their expression pattern. It seems possible, therefore, that *Pax3* may function upstream in the PDGFα/PDGFRα signalling pathway. In support of this idea, double mutants for *Patch* (which have deletions encompassing the *PDGFRα* gene) and *splotch* have been shown to exhibit a phenotype that is no more severe than the single mutants (Mark Mercola, personal communication), consistent with the idea that both genes may act in the same genetic pathway.

### *Anterior–Posterior Disorganisation of the Somite in the $Sp^{2H}$ Mutant*

In contrast to the rib truncations seen in *Myf5* null embryos, several mouse mutants show rib fusions and bifurcations (e.g., null mutants for *PDGFRα* and *paraxis*). These defects vary in severity, from minor fusions/bifurcations at the end of the ribs to major fusions spanning several ribs (Burgess *et al.,* 1996; Soriano, 1997). Mice lacking *paraxis* show severe rib fusions and bifurcations and lack the normal flexure of the vertebral column. In addition, these foetuses also show absent or hypotrophic limb, intercostal, and body wall muscles (Burgess *et al.,* 1996), all of which are reminiscent of the defects we find in the $Sp^{2H}$ mutant. *Pax3* and *paraxis* are initially induced independent of one another, as each is expressed in the other's absence. In $Sp^{2H}$ homozygotes, however, *paraxis* expression is lost with a striking absence of the rostrocaudal definition of the somite boundaries. This suggests a role for *Pax3* in maintaining *paraxis* expression during segmentation of the body axis. Conversely, the expression domain of *PDGFRα* and other genes such as *versican* is expanded in $Sp^{2H}$ mutants, with expression in both rostral and caudal parts of the somite (Henderson *et al.,* 1997; Soriano, 1997). These findings suggest that *Pax3* may regulate, either positively or negatively, the rostrocaudal expression of a number of downstream genes, which themselves may have roles in anteroposterior organisation of the body axis. Fusions of rib, neural arch, and intercostal muscles may therefore be a direct consequence of this loss of anteroposterior organisation and the loss of defined somite boundaries as shown by loss of *paraxis* expression. Rib and intercostal muscle precursors in the ventrolateral part of the somite may have lost specific guidance cues. This is supported by the presence of *myogenin*-expressing cells outside the myotome in $Sp^{2H}/Sp^{2H}$ embryos. Alternatively, the loss of normal anteroposterior organisation of the somite might result in formation of ribs, not only from the caudal part of the somite where they normally arise, but also from the rostral part, resulting in fusion of adjoining elements.

*Pax3* is the closest vertebrate homologue of the *Drosophila paired* gene, which is expressed in a dynamic pattern during *Drosophila* embryogenesis (Gutjahr *et al.,* 1993) and is involved in specification of stripes of expression of downstream genes such as *engrailed, hedgehog,* and *gooseberry*. When *paired* is expressed ectopically, the expression domains of downstream genes are expanded posteriorly (Miskiewicz *et al.,* 1996). This might, therefore, reflect some functional conservation between *Pax3* and *paired* in defining the posterior domains of body segments.

## ACKNOWLEDGMENTS

We are grateful to the British Heart Foundation and the Wellcome Trust who provided financial support for this study.

## REFERENCES

Beechey, C. V., and Searle, A. G. (1986). Mutations at the *Sp* locus. *Mouse News Lett.* **75,** 28.

Bober, E., Franz, T., Arnold, H.-H., Gruss, P., and Tremblay, P. (1994). *Pax-3* is required for the development of limb muscles: A possible role for the migration of dermomyotomal muscle progenitor cells. *Development* **120,** 603–612.

Braun, T., Rudnicki, M. A., Arnold, H.-H., and Jaenisch, R. (1992). Targeted inactivation of the muscle regulatory gene *Myf-5* results in abnormal rib development and perinatal death. *Cell* **71,** 369–382.

Burgess, R., Cserjesi, P., Ligon, K. L., and Olson, E. N. (1995). Paraxis: A basic helix-loop-helix protein expressed in paraxial mesoderm and developing somites. *Dev. Biol.* **168,** 296–306.

Burgess, R., Rawls, A., Brown, D., Bradley, A., and Olson, E. N. (1996). Requirement of the *paraxis* gene for somite formation and musculoskeletal patterning. *Nature* **384,** 570–573.

Chalepakis, G., Stoykova, A., Wijnholds, J., Tremblay, P., and Gruss, P. (1993). Pax: Gene regulators in the developing nervous system. *J. Neurobiol.* **24,** 1367–1384.

Christ, B., and Ordahl, C. P. (1995). Early stages of chick somite development. *Anat. Embryol.* **191,** 381–396.

Christ, B., Schmidt, C., Huang, R., Wilting, J., and Brand-Saberi, B. (1998). Segmentation of the vertebrate body. *Anat. Embryol.* **197,** 1–8.

Conway, S. J., Henderson, D. J., Anderson, R. H., Kirby, M. L., and Copp, A. J. (1997a). Development of a lethal congenital heart defect in the *splotch* (*Pax3*) mutant mouse. *Cardiovasc. Res.* **36,** 163–173.

Conway, S. J., Henderson, D. J., and Copp, A. J. (1997b). *Pax3* is required for cardiac neural crest migration in the mouse: Evidence from the *splotch* ($Sp^{2H}$) mutant. *Development* **124,** 505–514.

Cossu, G., Kelly, R., Tajbakhsh, S., Di Donna, S., Vivarelli, E., and Buckingham, M. (1996). Activation of different myogenic pathways: Myf-5 is induced by the neural tube and MyoD by the dorsal ectoderm in mouse paraxial mesoderm. *Development* **122,** 429–437.

Cserjesi, P., Brown, D., Ligon, K. L., Lyons, G. E., Copeland, N. G., Gilbert, D. J., Jenkins, N. A., and Olson, E. N. (1995). Scleraxis: A basic helix-loop-helix protein that prefigures skeletal formation during mouse embryogenesis. *Development* **121,** 1099–1110.

Daston, G., Lamar, E., Olivier, M., and Goulding, M. (1996). *Pax-3* is necessary for migration but not differentiation of limb muscle precursors in the mouse. *Development* **122,** 1017–1027.

Deutsch, U., Dressler, G. R., and Gruss, P. (1988). Pax 1, a member of a paired box homologous murine gene family, is expressed in segmented structures during development. *Cell* **53,** 617–625.

Epstein, D. J., Malo, D., Vekemans, M., and Gros, P. (1991a). Molecular characterization of a deletion encompassing the splotch mutation on mouse chromosome 1. *Genomics* **10,** 89–93.

Epstein, D. J., Vekemans, M., and Gros, P. (1991b). splotch ($Sp^{2H}$), a mutation affecting development of the mouse neural tube, shows a deletion within the paired homeodomain of Pax-3. *Cell* **67,** 767–774.

Fan, C.-M., and Tessier-Lavigne, M. (1994). Patterning of mammalian somites by surface ectoderm and notochord: Evidence for sclerotome induction by a hedgehog homolog. *Cell* **79,** 1175–1186.

Franz, T. (1992). Neural tube defects without neural crest defects in Splotch mice. *Teratology* **46,** 599–604.

Franz, T., Kothary, R., Surani, M. A. H., Halata, Z., and Grim, M. (1993). The Splotch mutation interferes with muscle development in the limbs. *Anat. Embryol.* **187,** 153–160.

Goulding, M., Lumsden, A., and Paquette, A. J. (1994). Regulation of *Pax-3* expression in the dermomyotome and its role in muscle development. *Development* **120,** 957–971.

Goulding, M. D., Chalepakis, G., Deutsch, U., Erselius, J. R., and Gruss, P. (1991). Pax-3, a novel murine DNA binding protein expressed during early neurogenesis. *EMBO J.* **10,** 1135–1147.

Grass, S., Arnold, H. H., and Braun, T. (1996). Alterations in somite patterning of *Myf-5*-deficient mice: A possible role for FGF-4 and FGF-6. *Development* **122,** 141–150.

Gutjahr, T., Frei, E., and Noll, M. (1993). Complex regulation of early paired expression: Initial activation by gap genes and pattern modulation by pair-rule genes. *Development* **117,** 609–623.

Henderson, D. J., Ybot-Gonzalez, P., and Copp, A. J. (1997). Overexpression of the chondroitin sulphate proteoglycan *versican* is associated with defective neural crest migration in the *Pax3* mutant mouse (*splotch*). *Mech. Dev.* **69,** 39–51.

Huang, R., Zhi, Q., Wilting, J., and Christ, B. (1994). The fate of somitocoele cells in avian embryos. *Anat. Embryol.* **190,** 243–250.

Kato, N., and Aoyama, H. (1998). Dermomyotomal origin of the ribs as revealed by extirpation and transplantation experiments in chick and quail embryos. *Development* **125,** 3437–3443.

Kawasaki, E. S. (1990). "PCR Protocols: A Guide to Methods and Applications." Academic Press, New York.

Maroto, M., Reshef, R., Münsterberg, A. E., Koester, S., Goulding, M., and Lassar, A. B. (1997). Ectopic *Pax-3* activates *Myo-D* and *Myf-5* expression in embryonic mesoderm and neural tissue. *Cell* **89,** 139–148.

Miskiewicz, P., Morrissey, D., Lan, Y., Raj, L., Kessler, S., Fujioka, M., Goto, T., and Weir, M. (1996). Both the paired domain and homeodomain are required for in vivo function of *Drosophila* Paired. *Development* **122,** 2709–2718.

Neubüser, A., Koseki, H., and Balling, R. (1995). Characterization and developmental expression of *Pax9*, a paired-box-containing gene related to *Pax1*. *Dev. Biol.* **170,** 701–716.

Ordahl, C. P., and Le Douarin, N. M. (1992). Two myogenic lineages within the developing somite. *Development* **114,** 339–353.

Orr-Urtreger, A., and Lonai, P. (1992). Platelet-derived growth factor-A and its receptor are expressed in separate, but adjacent cell layers of the mouse embryo. *Development* **115,** 1045–1058.

Rudnicki, M. A., and Jaenisch, R. (1995). The MyoD family of transcription factors and skeletal myogenesis. *Bioessays* **17,** 203–209.

Smith, T. H., Kachinsky, A. M., and Miller, J. B. (1994). Somite subdomains, muscle cell origins, and the four muscle regulatory factor proteins. *J. Cell Biol.* **127,** 95–105.

Soriano, P. (1997). The PDGF$\alpha$ receptor is required for neural crest cell development and for normal patterning of the somites. *Development* **124,** 2691–2700.

Tajbakhsh, S., Rocancourt, D., Cossu, G., and Buckingham, M. (1997). Redefining the genetic hierarchies controlling skeletal myogenesis: *Pax-3* and *Myf-5* act upstream of *MyoD*. *Cell* **89,** 127–138.

Tajbakhsh, S., and Spörle, R. (1998). Somite development: Constructing the vertebrate body. *Cell* **92,** 9–16.

Timmons, P. M., Wallin, J., Rigby, P. W. J., and Balling, R. (1994). Expression and function of *Pax 1* during development of the pectoral girdle. *Development* **120,** 2773–2785.

Tremblay, P., Dietrich, S., Mericskay, M., Schubert, F. R., Li, Z., and Paulin, D. (1998). A crucial role for Pax3 in the development of the hypaxial musculature and the long-range migration of muscle precursors. *Dev. Biol.* **203,** 49–61.

Tucker, R. P., Hammarback, J. A., Jenrath, D. A., Mackie, E. J., and Xu, Y. (1993). Tenascin expression in the mouse: In situ localization and induction in vitro by bFGF. *J. Cell Sci.* **104,** 69–76.

Wang, Y., Schnegelsberg, P. N. J., Dausman, J., and Jaenisch, R. (1996). Functional redundancy of the muscle-specific transcription factors Myf5 and myogenin. *Nature* **379,** 823–825.

Wilkinson, D. G. (1992). "In Situ Hybridisation: A Practical Approach." IRL Press, Oxford.

Received for publication September 30, 1998
Revised January 6, 1999
Accepted January 20, 1999